physica status solidi b
www.pss-b.com

Structural, Elastic, Electronic, Magnetic, and Thermoelectric Characteristics of $MgEu_2X_4$ (X = S, Se) Spinel Compounds: Ab-Initio Calculations

Ahmad A. Mousa, Said M. Al Azar, Saber Sâad Essaoud, Khadidja Berarma, Aymen Awad, Nada T. Mahmoud, Emad K. Jaradat, and Mohammed S. Abu-Jafar*

The structural, elastic, electronic, magnetic, and thermoelectric properties of $MgEu_2X_4$ (X = S and Se) spinel compounds are investigated computationally. Calculations are performed using the full-potential linearized augmented plane wave (FP-LAPW) method within the Perdew, Burke, and Ernzerhof generalized gradient approximation (PBE-GGA), GGA + U, and modified Becke–Johnson (mBJ-GGA) approximations. The band structure and density of states results from the three exchange-correlation approximation methods (mBJ, GGA + U, and PBE) show that these spinel compounds are fully spin-polarized. Also, they possess a half-metallic character in the spin-down channel with a direct bandgap (Γ–Γ) of about 3.44, 2.712, and 2.472 eV for $MgEu_2S_4$ and 2.89, 2.285, and 2.017 eV for $MgEu_2Se_4$, respectively. The formation of both compounds is energetically favorable based on the results of the total energy and cohesive energy calculations. Furthermore, the two compounds are chemically and mechanically stable, as concluded from cohesive energy and elastic calculations. The elastic calculations reveal that both spinel compounds are ductile materials. The ionic bonds are predominant. The quasi-harmonic model has also been used to investigate the influences of temperature and pressure on thermal characteristics. The thermoelectric behavior is studied using the BoltzTraP code. Both systems show good thermoelectric properties for the spin-down channel.

1. Introduction

In materials science, spinel compounds play a significant role; owing to their potential applications in device fabrication, considerable research interest has been devoted both from academia and industry.[1–3] The spinel compounds are a series of minerals having the general formula $X^{II}Y_2^{II,III}Z_4^{VI}$. They crystallize in the cubic crystal structure. The anions (Z^{VI}) are arranged in a cubic closed-packed lattice while the cations (X^{II} and $Y^{II,III}$) occupy some or all of the lattice's octahedral and tetrahedral positions.[4] Wang et al[5] investigated the elastic and electronic properties of 30 AB_2X_4 spinel compounds (A = Be, Mg, Ca, Sr, Ba; B = Al, Ga, In; X = O, S). They highlighted the influence of cation and anion variance on the above-mentioned properties. Some correlations between lattice constants, bulk modulus, ionic radii, and electromagnetism of constituent ions were identified.

The significance of this research stems from the fact that it will shed more light on the well-known properties of spinel that could be employed in diverse scientific and technological fields. The novelty of this work principally anchors on finding and proving the half-metallic ferromagnetic character of $MgEu_2S_4$ and $MgEu_2Se_4$ Spinel compounds. The half-metallic compounds are technologically attractive; as they have wide technological applications in spintronics, thermoelectric and optoelectronic devices. These studied compounds can be used for further experimental investigations in spintronics and optoelectronics. In addition, we have found that the two compounds are mechanically stable, as concluded from elastic calculations. Recently, Koettgen et al. investigated

A. A. Mousa
Department of Basic Sciences
Middle East University
Amman 11831, Jordan

S. M. Al Azar
Department of Physics
Faculty of Science
Zarqa University
Zarqa 13132, Jordan
E-mail: salazar@zu.edu.jo

The ORCID identification number(s) for the author(s) of this article can be found under https://doi.org/10.1002/pssb.202200191.

DOI: 10.1002/pssb.202200191

S. S. Essaoud
Department of Physics
University of M'sila
28000 M'sila, Algeria

S. S. Essaoud
Laboratoire de Physique des Particules et Physique Statistique
Ecole Normale Supérieure-Kouba
BP 92, Vieux-Kouba, 16050 Algiers, Algeria

K. Berarma
Department of Chemistry
University of M'sila
28000 M'sila, Algeria

computationally seven $MgLn_2X_4$ (Ln = lanthanoid, X = S, Se) chalcogenide spinels to calculate Mg^{2+} mobility and stability.[6] They concluded that the size of the cation decreases the Mg ion migration barrier, but this leads to a decrease in the stability, and the non-spinel structures are favored. These interesting results encourage the possibility to find similar behaviors in associated crystal structures. Mg-based spinels could be promised materials for batteries, thermoelectric, and optoelectronics applications and this motivates more research to find new suitable materials. Also, nanoparticles of spinel ferrite have received considerable attention among researchers due to their widespread technological applications such as magnetic resonance imaging (MRI) contrast agent, drug-delivery, magnetically recoverable efficient photo-catalyst, gas sensor, hyperthermia cancer treatment, magnetic refrigeration (MR), anode material for Li-ion battery, magnetic recording media with higher storage density, microwave devices, spintronic devices, super-capacitors, paint industry, water splitting for hydrogen production, etc.[5,7] Idrissi et al recently studied the physical properties of $NiFe_2O_4$[8] and $ZnFe_2O_4$[9] spinels using density functional theory (DFT), Monte Carlo simulation, and mean-field theory. They found that $NiFe_2O_4$ spinel shows a second-order ferromagnetic-paramagnetic phase transition around $T_c = 844$ K and this result is in good agreement with the experiment. Jebari et al. investigated theoretically the electronic and magnetocaloric properties of the $Bi_{25}FeO_{40}$ compound.[10] It shows good magnetocaloric properties around T_c. Furthermore, many other studies on different spinel compounds have been carried out in extensive research using Monte Carlo simulations, first-principles calculations, mean-field, and series expansions to calculate magnetic properties as well as the nearest neighbor exchange interaction between atoms.[11–16]

In this study, we will investigate undoped magnetic semiconductors $MgEu_2X_4$ that have a periodic arrangement of magnetic elements on their own. Also, the europium chalcogenide spinels appeared as very exotic materials which motivated us for further investigations. The full-potential linearized augmented plane waves (FP-LAPW) method was used to determine the structural, elastic, electronic, and thermoelectric properties for $MgEu_2X_4$ (X = S and Se) spinel compounds. The following is the format of this article: Section two discusses computational approaches. Section three contains the results and discussion. Finally, Section four summarizes the major conclusions of this research.

2. Calculation Method

$MgEu_2X_4$ (X = S and Se) compounds have a cubic structure with a space group Fd-3m (#227). The self-consistent computations were carried out with the FP-LAPW technique,[17] which is based on DFT,[18] and Wien2k.[19] The unit cell of the crystal is divided into two sections in this method: the non-overlapping spheres (atomic spheres) and the interstitial region (the region outside the atomic spheres). Spherical harmonic functions inside the non-overlapping spheres encircling the atomic sites (muffin tin spheres) and a plane wave basis set in the remaining space of the unit cell increase the wave function, charge density, and potential (interstitial region). To derive the energy-volume relation, the calculated total energies are fitted to the Murnaghan equation of state.[20] The GGA-PBE,[21] Hubbard-like correction GGA + U,[22,23] and mBJ-GGA approaches[24] are used to treat the exchange-correlation potential.

For the Eu 4f states the value of the effective Hubbard interaction potential of 0.55 is used in GGA + U scheme. For a correlated system and for a full potential calculation, we used an effective Hubbard parameter defined as $U_{\text{eff}} = U - J$. It can be calculated with the augmented plane-wave methods. For the Eu 4f states, $U_{\text{eff}} = E_{4f\uparrow}\left(\frac{n+1}{2}, \frac{n}{2}\right) - E_{4f\uparrow}\left(\frac{n+1}{2}, \frac{n}{2} - 1\right) - E_{\text{F}}\left(\frac{n+1}{2}, \frac{n}{2}\right) - E_{\text{F}}\left(\frac{n+1}{2}, \frac{n}{2} - 1\right)$, where n is the orbital occupation number. The Eu 4f states lead to the value of 0.038 Ry for the calculated J constant. Combined with the value of 0.59 Ry for the Hubbard parameter, it leads to the effective Hubbard potential of 0.549 Ry (7.48 eV) for both compounds.[25]

The wave-function expansion inside the atomic spheres has a maximum quantum number of $l_{\max} = 10$. For the expansion of wavefunctions in the interstitial area, the core cutoff energy of 81.66 eV, and the plane wave cutoff $K_{\max} = 8/R_{\text{mt}}$ are used (R_{mt} is the lowest muffin-tin radius in the unit cell, and $K_{\max}$ is the magnitude of the biggest **K** vector in the plane-wave expansion).

The R_{mt} values for Mg, Eu S, and Se atoms are 2.2, 2.5, 2.2, and 2.4a.u., respectively. For all compounds, the Brillouin zone integrations within the self-consistency cycle are done using a tetrahedron method, which uses the 56 k-points in the irreducible wedge of the irreducible Brillouin zone (IBZ). The self-consistence calculations are considered converged when the force and charge convergence tolerances are less than 0.1mRy $a.u^{-1}$ and 1 m electron charges, respectively.

K. Berarma
Laboratory of Inorganic Materials
Department of Chemistry
University of M'sila
28000 M'sila, Algeria

A. Awad
Department of Civil Engineering
Middle East University
Amman 11831, Jordan

N. T. Mahmoud
Physics Department
The University of Jordan
11942 Amman, Jordan

E. K. Jaradat
Department of Physics
Mutah University
61710 Karak, Jordan

M. S. Abu-Jafar
Department of Physics
An-Najah National University
7 Nablus, Palestine

3. Results and Discussion

3.1. Structural Properties and Cohesion Energies

In this subsection, we investigate the structural parameters and cohesive energies for $MgEu_2X_4$ (X = S and Se) spinel compounds. The cubic spinel structure of $MgEu_2X_4$ (X = S, Se) compounds used in this study is shown in **Figure 1**. Murnaghan's equation of state (EOS) has been used to fit the obtained data and to calculate the equilibrium volume, lattice constant (a), bulk modulus (B), and first pressure derivative (B').[20] **Figure 2** shows the relationship between the total energy of the compound versus its volume. Our results with available previous studies are listed in **Table 1**. The equilibrium lattice parameters for both compounds are within accepted differences from the previous values.[4] To our knowledge, this study is the first detailed study of $MgEu_2X_4$ (X = S, Se) spinel structures; Therefore, it is difficult to compare the results with previous studies.

The cohesive energy (E_{coh}) is one of the most important indicators of the stability of the compounds in their ground state, where it is the energy that must be supplied to the solid to separate its constituents into neutral free atoms. The negative value of the cohesive energy is an indication of the chemical stability of the compound. The cohesive energy (E_{coh}) is defined as[26,27]

$$E_{coh} = E_{tot}^{MgEu_2X_4} - (E_{Mg}^{atom} + 2E_{Eu}^{atom} + 4E_{X}^{atom}) \quad (1)$$

where $E_{tot}^{MgEu_2X_4}$ represents the total bulk energy of $MgEu_2X_4$ (X = S, Se) compounds in the cubic structure and E_{Mg}^{atom}, E_{Eu}^{atom}, E_{X}^{atom} are the energies of Mg, Eu, and (X = S, Se) as isolated atoms, respectively. The calculated values of cohesive energies are listed in Table 1. Both compounds' cohesive energy values are obviously negative; thus, we draw the conclusion that they are chemically stable.

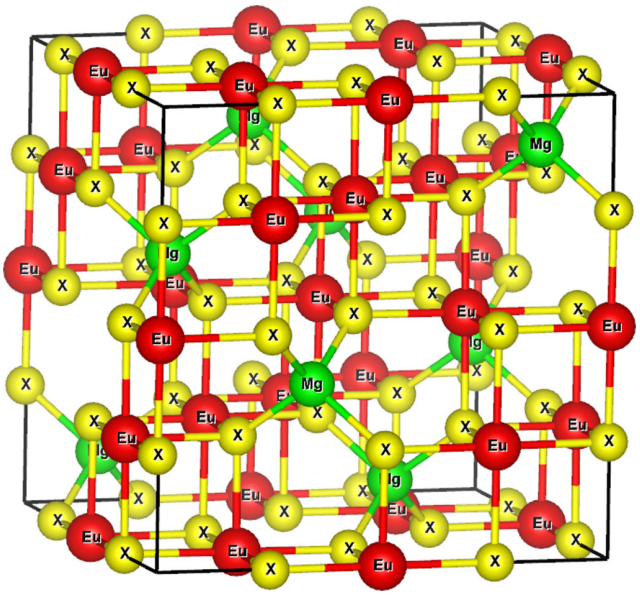

Figure 1. Crystal structure of $MgEu_2X_4$ (X = S, Se) spinel compounds.

3.2. Elastic Properties

In material research, estimating elastic and mechanical characteristics is critical for process control and formation. The IRelast package[28,29] was used to calculate elastic and mechanical characteristics. Cubic crystal symmetry necessitates the calculation of three independent elastic constants, C_{11}, C_{12}, and C_{44}, to determine the system's characteristics. The elastic constants for $MgEu_2X_4$ (X = S and Se) spinel compounds are listed in **Table 2**.

One can tell whether a compound is mechanically stable or not by looking at the single-crystal constants. Born and Huang[30] provide three widely recognized elastic stability criteria for cubic crystals: $C_{11} > 0$, $C_{11} - C_{12} > 0$, $C_{11} + 2C_{12} > 0$, $C_{44} > 0$. From Table 2, it is noticed that the results of the elastic constants for $MgEu_2S_4$ and $MgEu_2Se_4$ compounds satisfy the above-mentioned stability criteria, ensuring their respective mechanical stability. However, no study has reported or compared the elastic constant calculations for $MgEu_2S_4$ and $MgEu_2Se_4$ compounds in the literature. Therefore, this research may serve as inspiration for other researchers.

In contrast, and as expected, Table 2 shows the agreement of the values of the bulk modulus calculated from the elastic constants ($B = \frac{C_{11}+2C_{12}}{3}$) with the one calculated using Murnaghan's equation (in the structural properties subsection). Both compounds have low bulk modulus, which corresponds to less volumetric resistance to compression.

The anisotropy factor $A = 2C_{44}/(C_{11}-C_{12})$ was used to count the elastic anisotropy of $MgEu_2S_4$ and $MgEu_2Se_4$ compounds. This factor has significant implications for engineering research since it is linked to the ability to create micro-cracks in materials, with micro-cracks being the tiniest component of the failure chain.[31–34] These cracks become more important if they start to run together and form a failure pattern. For an isotropic crystal, A equals one, but any deviation from one indicates anisotropy behavior. Table 2 shows that $MgEu_2S_4$ and $MgEu_2Se_4$ compounds have elastic anisotropy.

The Voigt–Reuss–Hill (VRH) method can be used to calculate the shear modulus (S) using elastic constants.[35–37] The Hill shear modulus S_H is calculated as follows

$$S_H = \frac{1}{2}(S_V + S_R) \quad (2)$$

where S_V and S_R are the Voigt and Reuss shear moduli, respectively. We can come up with these moduli by utilizing the following formulas

$$S_V = \frac{1}{5}(C_{11} - C_{12} + 3C_{44}) \quad (3)$$

$$S_R = \frac{5C_{44}(C_{11} - C_{12})}{4C_{44} + 3(C_{11} - C_{12})} \quad (4)$$

The bulk modulus B and the shear modulus S_H are connected to Poisson's ratio ν, and Young's modulus Y via the following equations

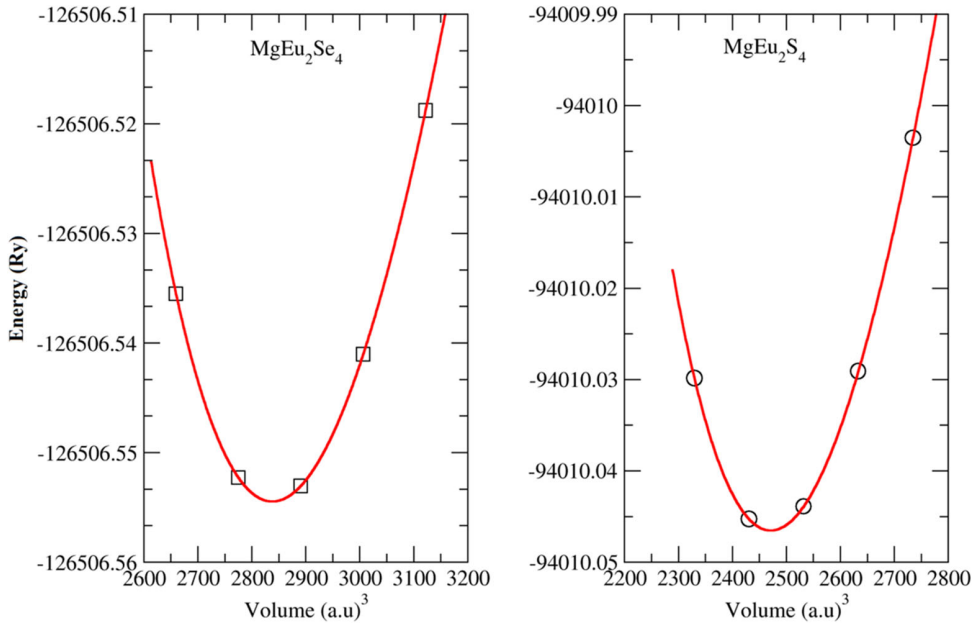

Figure 2. The total energy values as a function of unit cell volumes for the $MgEu_2X_4$ (X = S, Se) spinel compounds.

Table 1. Lattice constant (a), bulk modulus (B), and cohesive energy (E_{coh}) of $MgEu_2S_4$ and $MgEu_2Se_4$ spinel compounds.

–	a [Å]	B [GPa]	E_{coh} [Ry]
$MgEu_2S_4$	11.356	54.1	−2.82
	11.420[4]	–	–
$MgEu_2Se_4$	11.893	43.9	−2.22
	11.959[4]	–	–

$$Y = \frac{9BS_H}{3B + S_H}, \quad \nu = \frac{3B - 2S_H}{6B + 2S_H} \tag{5}$$

Table 2 summarizes the results of these parameters for the $MgEu_2X_4$. According to our knowledge, there are no previous studies for these compounds' elastic constants, thus according to our belief, this is the first theoretical prediction of these quantities. The material hardness can be measured using Young's modulus and the shear modulus.[38] When the S_H and Y values are increased, the materials get stiffer in general. The obtained values of these moduli suggest that $MgEu_2S_4$ is stiffer than $MgEu_2Se_4$.

The ratio of the bulk modulus to the shear modulus, B/S_H, an empirical relationship relating to the elastic properties of the material, is used to characterize the brittle and ductile behaviors of a material. A high B/S_H value is connected with ductility, while a low value is associated with brittleness, according to the Pugh ratio.[39] The critical value of the Pugh ratio that distinguishes between the two behavior is identified as 1.75. Table 2 clearly shows that the B/S_H ratio of $MgEu_2X_4$ compounds is greater than the threshold value of 1.75, indicating that both $MgEu_2S_4$ and $MgEu_2Se_4$ compounds are ductile. We also used Cauchy's pressure rule, which is defined as the difference between the elastic constants C_{12}–C_{44},[40] to determine if the materials were ductile or brittle. If Cauchy's pressure is positive (negative), the material will be ductile (brittle), according to this rule. Table 2 shows that Cauchy's pressure is positive for both compounds, indicating that they are both ductile. Also, the Poisson ratio (ν) can be used to calculate the ductility and brittleness of the material, where if the Poisson ratio exceeds 0.26, the material will be ductile, otherwise, it will be brittle.[41] From Table 2, the Poisson ratios are 0.277 and 0.284 for $MgEu_2S_4$ and $MgEu_2Se_4$, respectively, this means that both compounds are ductile. These results are compatible with those obtained by B/S_H ratio and Cauchy's pressure rule.

In contrast, the Poisson ratio (ν) can be used to forecast the type of chemical bonding. Poisson ratio is approximately equivalent to 0.25 or more for ionic materials, while it is less than 0.25 for covalent materials.[42] Table 2 lists the values of ν for $MgEu_2S_4$ and $MgEu_2Se_4$ (0.277 and 0.284 respectively), and the calculations demonstrate that $\nu > 0.25$, indicating an ionic bonding nature.

Table 2. Calculated elastic properties for $MgEu_2S_4$ and $MgEu_2Se_4$ spinel compounds.

–	C_{11} [GPa]	C_{12} [GPa]	C_{44} [GPa]	B [GPa]	S_H [GPa]	A (anisotropy)	Young's modulus	Poisson's ratio	B/S_H	$C_{12} - C_{44}$
$MgEu_2S_4$	107.922	30.339	24.367	56.200	29.381	0.628	75.061	0.277	1.913	5.972
$MgEu_2Se_4$	92.041	24.929	18.967	47.300	23.881	0.565	61.324	0.284	1.981	5.962

3.3. Electronic Structure and Magnetic Properties

In this subsection, the electronic structure and magnetic properties for both $MgEu_2S_4$ and $MgEu_2Se_4$ spinels will be discussed. The spin-polarized density of states (DOS) and band structure calculations of both $MgEu_2S_4$ and $MgEu_2Se_4$ are performed using GGA-PBE, GGA-mBJ, and GGA + U schemes at their equilibrium ferromagnetic lattice parameters. The spin-polarized band structure combined with corresponding atom-resolved DOS for both $MgEu_2S_4$ and $MgEu_2Se_4$ spinels is plotted in **Figures 3** and **4**, respectively. Both spinel's band structure and DOS show that they possess a half-metallic character. They form a direct ($\Gamma - \Gamma$) energy bandgap (E_g) in the minority channel (spin down), which possesses the values 3.44, 2.712, and 2.472 eV for $MgEu_2S_4$ and 2.893, 2.285, and 2.017 eV for $MgEu_2Se_4$ when the exchange-correlation potential was treated using different approximation schemes: GGA-mBJ, GGA + U, and GGA-PBE, respectively, as tabulated in **Table 3**. After bonding, each Eu atom loses three electrons and becomes Eu^{+3} with an f^6 electron configuration. The 4f electrons occupy gradually the majority spin t_{1g} states, thus the total magnetic moment increases. Indeed, the 4*f* states show a large spin exchange splitting and a small crystal field splitting. Our results of the band structure and the energy bandgap for both compounds contradict the literature, where the GGA-mBJ method gives a wider band gap than the GGA + U method for localized 4*f* state. The effect of the additional orbital-dependent Coulomb term was shifting upward the occupied and unoccupied 4*f* orbital rather than splitting between them. Furthermore, in the case of $MgEu_2Se_4$ using the GGA + U approximation makes some bands cross the Fermi level and form a pseudo-gap. The total DOS for both compounds show the existence of a large exchange splitting between majority and minority spin states illustrating the half-metallic feature for both spinel compounds.

The two band structures show bimodal ($Eu - 4f$) peaks near the Fermi level in the majority channel (spin up) which form flat bands. These structures appear clearer in the $MgEu_2Se_4$ spinel than $MgEu_2S_4$ spinel. The important conclusion from this structure, the peak near the Fermi level at spin-up and the E_F fall in, is that both spinel compounds are hard to stable or hard to synthesize.

The spin-polarized total and partial DOS for $MgEu_2S_4$ and $MgEu_2Se_4$ spinels are plotted in **Figures 5** and **6**, respectively. The spin-projected DOS shows that the states above the Fermi level (at 2.5–5 eV) are primarily showing $Eu - 4f$ character peak. The states in (−4.5–0) eV are primarily composed of ($S - 3p/Se - 4p$) states with a considerable admixture of the $Eu - 4f$ orbitals at the upper band and ($Mg - 2s$)/($Mg - 2p$) orbitals at the lower band. This hybridization suggested a strong covalent bond. The states from −12 to −10 eV are primarily composed of ($S - 3s/Se - 4s$) states with an admixture of the ($Mg - 2p$) orbitals. These strong overlapping between Mg(2p)-S(3s)/Mg(2p)-Se(4s) orbitals demonstrate covalence bonding. The deepest valence states are from ($Eu - 5p$) orbitals (from −19 to −17 eV). The ($Eu - 4f$) spin-up orbitals show bimodal peaks near the Fermi level in both compounds. The ($Eu - 4f$) states are dominant around the Fermi level for both compounds. Also, the ($Mg - 3d$) states are empty and do not play a significant role in the gap established.

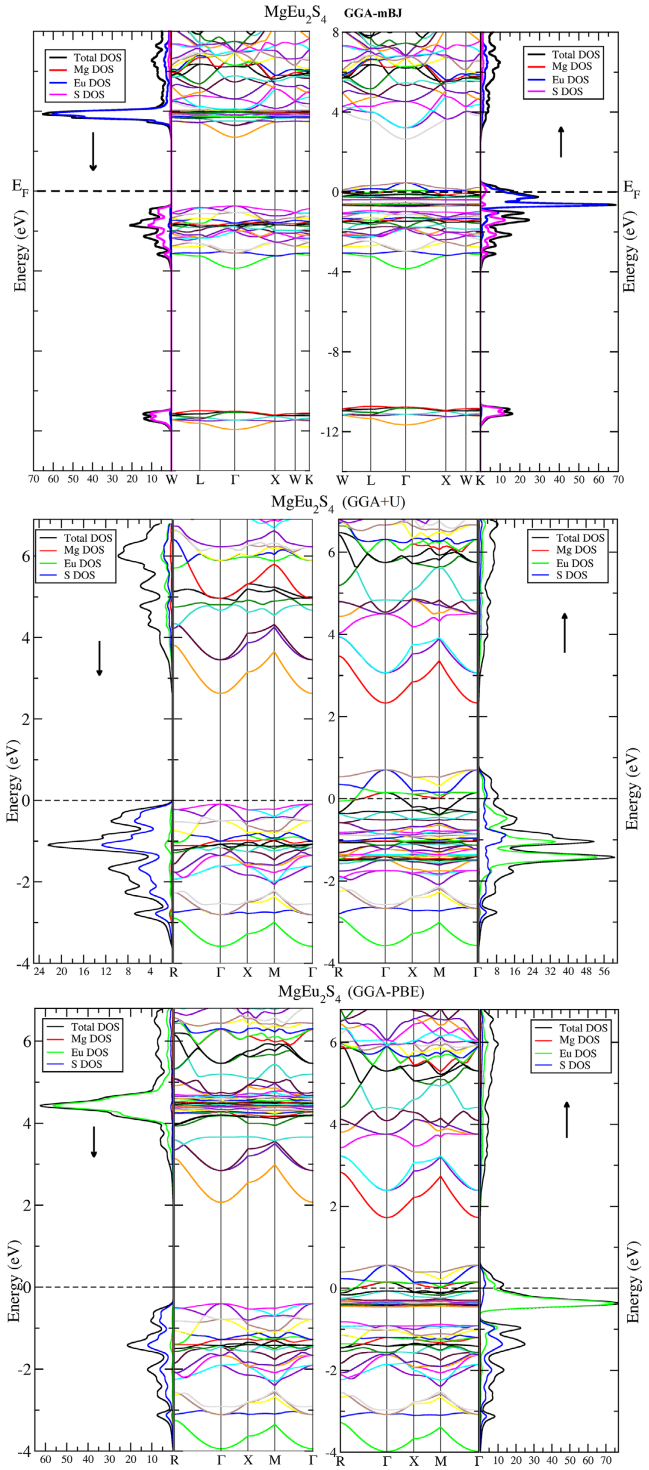

Figure 3. The spin-polarized band structure combined with its corresponding DOS for $MgEu_2S_4$ within generalized gradient approximation-modified Becke–Johnson (GGA-mBJ), GGA + U, and GGA Perdew, Burke, and Ernzerhof (PBE) approximations.

In Table 3, we display the calculated electronic and magnetic properties for both $MgEu_2S_4$ and $MgEu_2Se_4$ spinel compounds. According to our knowledge, there is no previous data to compare.

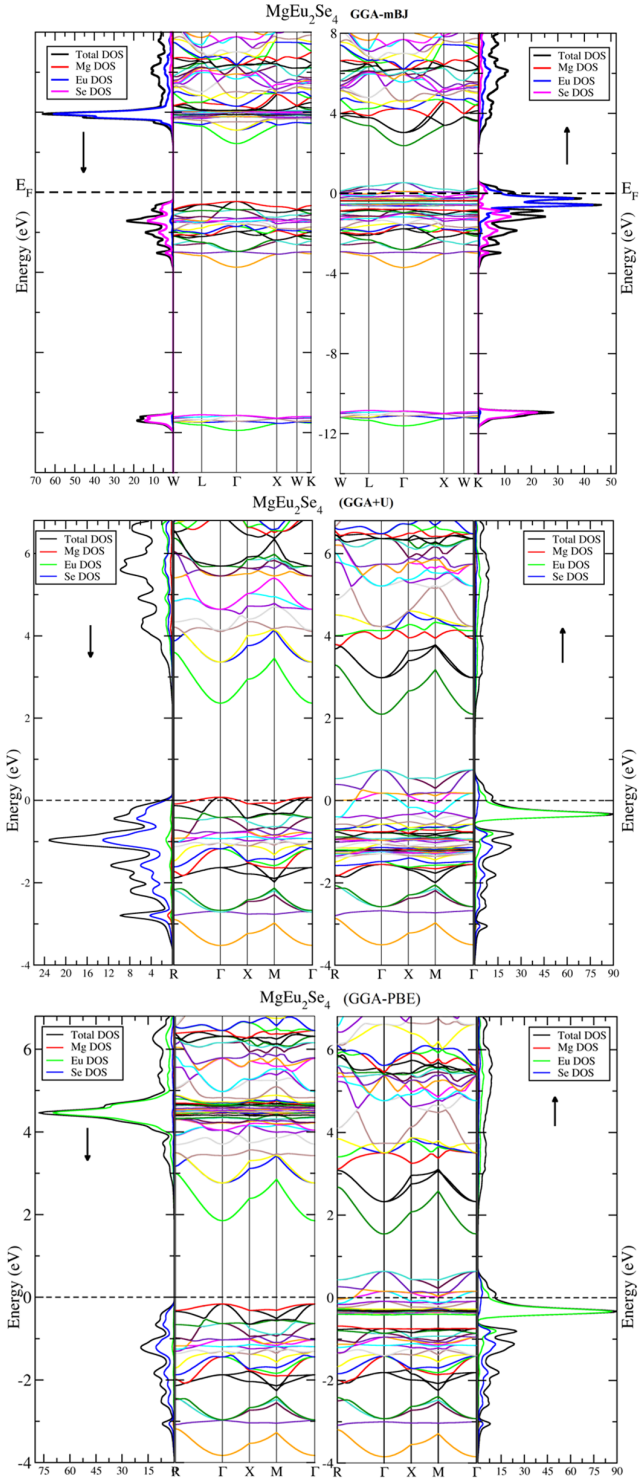

Figure 4. The spin-polarized band structure combined with its corresponding DOS for $MgEu_2Se_4$ within GGA-mBJ, GGA + U, and GGA- PBE approximations.

The two spinels have an open spin gap (E_s), the E_s as defined in ref.[43] is the energy difference between the E_F and the HOMO energy in the minority channel, and a full polarization also equal to the total spin magnetic moment which means that the chalcogen elements do not affect the total spin magnetic moment. The most of magnetic moment per cell comes from (localized in) europium atoms. This state was described in detail within the Heisenberg model framework. The opposite signs of the atom-resolved spin magnetic moment for Eu and chalcogens reveal that their valence bands interact antiferromagnetically. The electrons spin polarization is given by the relation $p = \frac{N_\uparrow(E_F) - N_\downarrow(E_F)}{N_\uparrow(E_F) + N_\downarrow(E_F)} \times 100\%$, where $N_\uparrow(E_F)/N_\downarrow(E_F)$ are spin-up/down DOS at E_F.[44] In our work, both spinels have integer total magnetic moment in GGA and $p = 100\%$ which obey Pauli–Slater behavior and confirm that they are full half-metal materials.

Table 3. The electric and magnetic properties for both $MgEu_2S_4$ and $MgEu_2Se_4$ spinel compounds.

	$MgEu_2S_4$			$MgEu_2Se_4$		
	mBJ	GGA + U	GGA	mBJ	GGA + U	GGA
LUMO [eV]	2.703	2.627	2.071	2.432	2.363	1.854
HOMO [eV]	−0.740	−0.092	−0.401	−0.460	0.077	−0.163
E_g [eV]	3.442	2.712	2.472	2.893	2.285	2.017
DOS(E_F)↑	110.44	106.44	115.73	150.82	141.91	127.46
DOS(E_F)↓	0	0	0	0	15.59	0
Spin polarization [%]	100	100	100	100	80	100
E_s [eV]	0.740	0.092	0.401	0.460	−0.077	0.163
MM_{TOT} [μ_B]	12.00	12.452	11.99	12.00	12.573	12.00
MM_{Mg} [μ_B]	0.005	−0.003	−0.002	0.005	−0.0052	−0.0037
MM_{Eu} [μ_B]	6.262	6.655	6.356	6.341	6.7208	6.4226
$MM_{S/Se}$ [μ_B]	−0.143	−0.285	−0.182	−0.173	−0.1996	−0.2008

3.4. Thermodynamic and Thermoelectric Characteristics

The effect of temperature on both thermodynamic and thermoelectric properties of $MgEu_2S_4$ and $MgEu_2Se_4$ is discussed in this section. In general, the impact of heat absorbed by crystalline materials causes a variety of phenomena on atoms and electrons inside the crystal lattice. The atoms forming solids vibrate around their equilibrium position as a result of gaining external thermal energy, so this energy is absorbed and stored. The value of the absorbed energy varies according to the heat capacity of the compound. The increase in temperature may generate an induced thermoelectric current caused by the movement of electrons, which contributes to the transfer of part of the heat. The thermal conductivity, heat capacity, and thermal expansion coefficient of lattices for $MgEu_2S_4$ and $MgEu_2Se_4$ compounds are pressure and temperature dependent. They are computed using Gibbs2 code[45,46] that is based on the quasi-harmonic Debye model.[47] The results are plotted in **Figure 7**.

The heat capacity of solid materials expresses the ability of a substance to absorb thermal energy. It increases with the increasing number of degrees of freedom of the particles.[48] The calculations conducted on the evolution of this property of both compounds at different temperatures and under the influence of external pressures with values 0, 10, and 20 GPa showed that it increases exponentially with $\approx T^3$ at low temperatures. In contrast, it converges toward the limits of Dulong–Petit limit

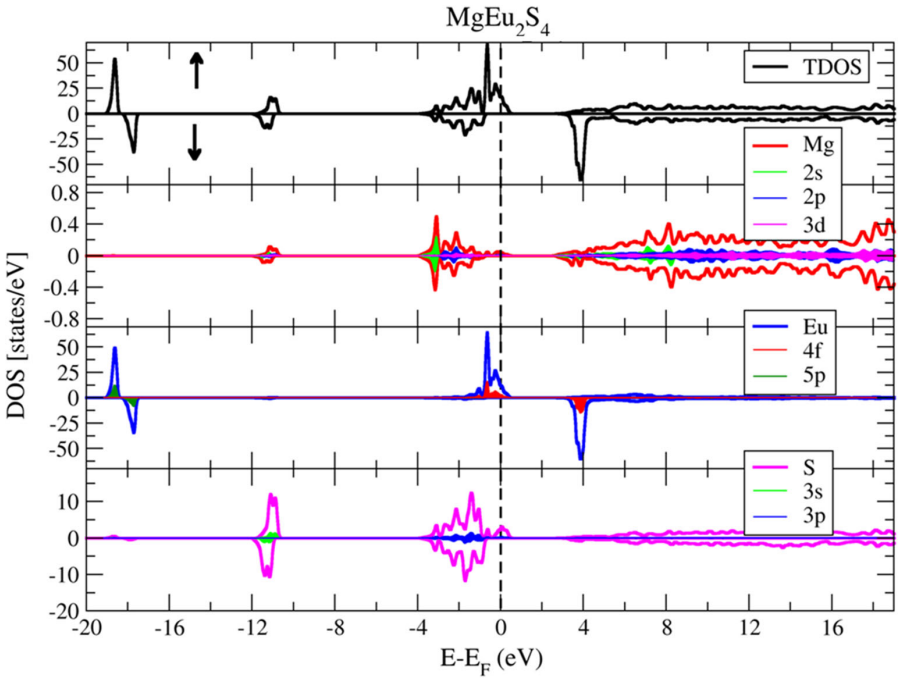

Figure 5. Spin-polarized total and partial DOS for cubic $MgEu_2S_4$ spinel compound.

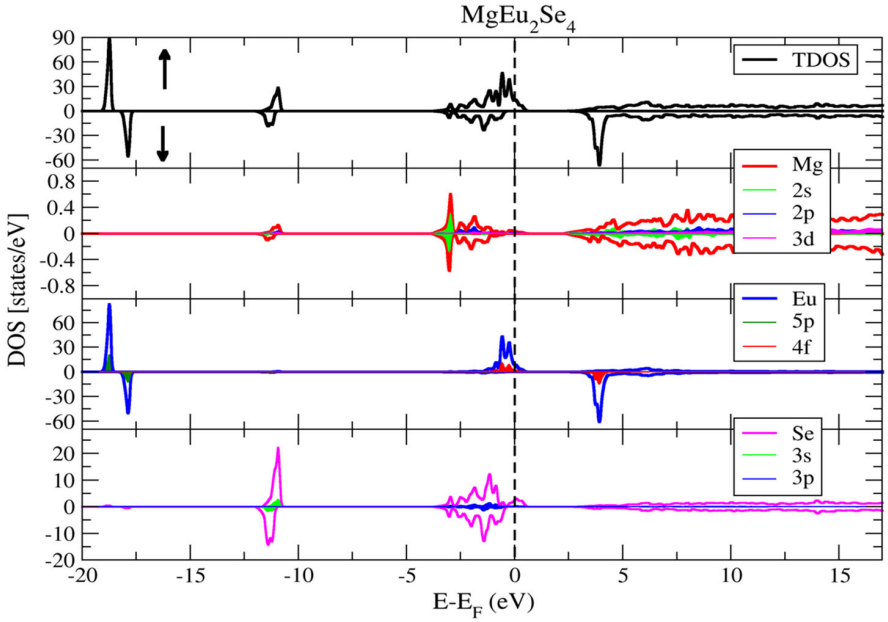

Figure 6. Spin-polarized total and partial DOS for cubic $MgEu_2Se_4$ spinel compound.

($Cv = 3NR$)[49] at high temperatures, for temperatures equal to or greater than 700 K for both compounds. At room temperature, we notice that the heat capacity of the $MgEu_2Se_4$ is greater than that of the $MgEu_2S_4$. Furthermore, it decreases with increasing external pressure.

The contribution of the lattice to the thermal conductivity κ_l can be estimated using the Slack model formula given by Ref. [50]: $\kappa_l = \frac{A\theta_D^3 V^{1/3} m}{\gamma^2 n^{2/3} T}$, where A is a physical constant equal to $A = \frac{2.4310^{-8}}{1-\frac{0.514}{\gamma}+\frac{0.228}{\gamma^2}}$ and θ_D, γ, V, n, and m are the Debye temperature, Grüneisen parameter, the volume per atom, the number of atoms in the primitive unit cell, and the average mass of all the atoms in the crystal, respectively. The findings revealed that the atoms of both compounds contribute significantly to heat transport at low temperatures, but even this contribution decreases dramatically as the temperature rises. The curves plotted in Figure 7 also show that the atoms of $MgEu_2S_4$ have a higher

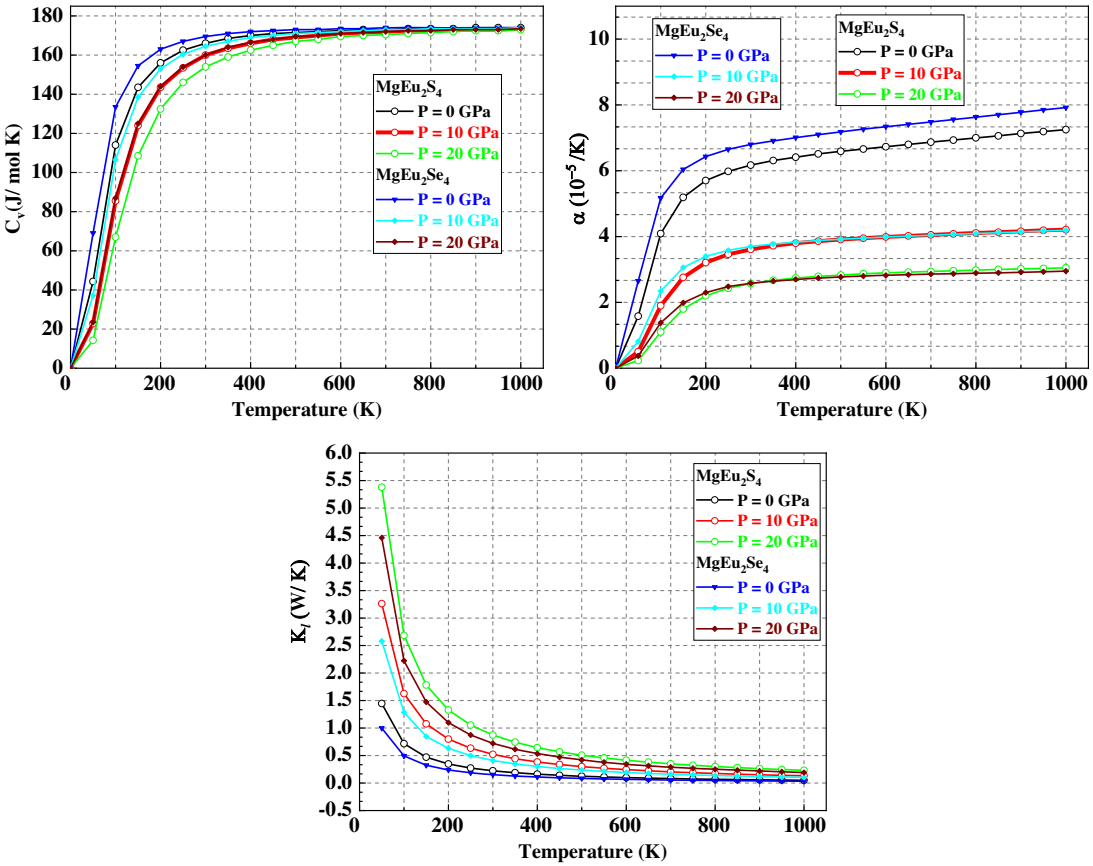

Figure 7. Pressure and temperature dependence of lattice thermal conductivity, heat capacity at volume constant, and the thermal expansion coefficient of $MgEu_2S_4$ and $MgEu_2Se_4$.

contribution to the lattice thermal conductivity than the atoms of $MgEu_2Se_4$ at the same pressure and temperature, as well as the direct proportionality between pressure and the lattice thermal conductivity of the crystal lattice, which seems that increasing the external pressure on the crystal lattice increases κ_l.

We have also plotted the variation of the thermal expansion coefficient for both compounds in terms of temperature at three pressures (0, 10, and 20 GPa), and we discovered that the $MgEu_2Se_4$ compound has a larger thermal expansion ability than $MgEu_2S_4$ at the same pressure and temperature, and that the thermal expansion coefficient of both compounds increases sharply at low temperatures (less than 150 K), as shown in Figure 7. In terms of the influence of external pressures on the coefficient of thermal expansion, we found that an increase in applied pressure reduces both compounds' thermal expansion ability.

The thermoelectric properties are explored for both compounds and in both spin channels up and down at different temperatures as a function of the relative chemical potential using the BoltzTraP program;[51] this code is based on the semiclassical Boltzmann theory. The first coefficient that has been studied is the Seebeck coefficient, which expresses the potential difference generated between the two ends of a substance when it is exposed to two different temperatures. As a first remark, we can easily observe through **Figure 8** that the Seebeck coefficient in the spin-down direction is larger than in the other case for both compounds with maxima of 3.0 mV K^{-1} at 300 K for $MgEu_2S_4$ and $MgEu_2Se_4$. In the case of spin-up orientation, the Seebeck coefficient of $MgEu_2S_4$ is higher than $MgEu_2Se_4$, and its value reaches 2.0 mV K^{-1} for the first compound at a temperature of 300 K. Also, we point out that the Seebeck coefficient affected directly by temperature changing and decreases with increasing temperature for both compounds and in both spins.

The electrical conductivity and electronic thermal conductivity have also been computed for both compounds in the majority and minority spin directions and plotted in Figure 8, as these two parameters are proportional to each other according to Weidman–Franz formula ($K_e = L\sigma T$ (where L is Lorentz number)), According to what has been indicated in these figures, we can notice that both compounds have a high electrical and thermal conductivity in the relative chemical potential range between −2.0 and −1.5 eV in both spin cases, in addition to the decrease in electrical and thermal conductivity with the increase in temperature.

Figure 9 shows the effect of temperature on the electronic heat capacity and the Pauli magnetic susceptibility. From this figure, we notice that each of these two coefficients has larger values in the case of spin up, unlike the other case, where both coefficients take low values, as for the electrical heat capacity, we notice that the $MgEu_2Se_4$ compound has a thermal electronic capacity greater than that of the $MgEu_2S_4$ compound, from where its maximum value is confined from −0.5 to 0 eV in the case of spin up

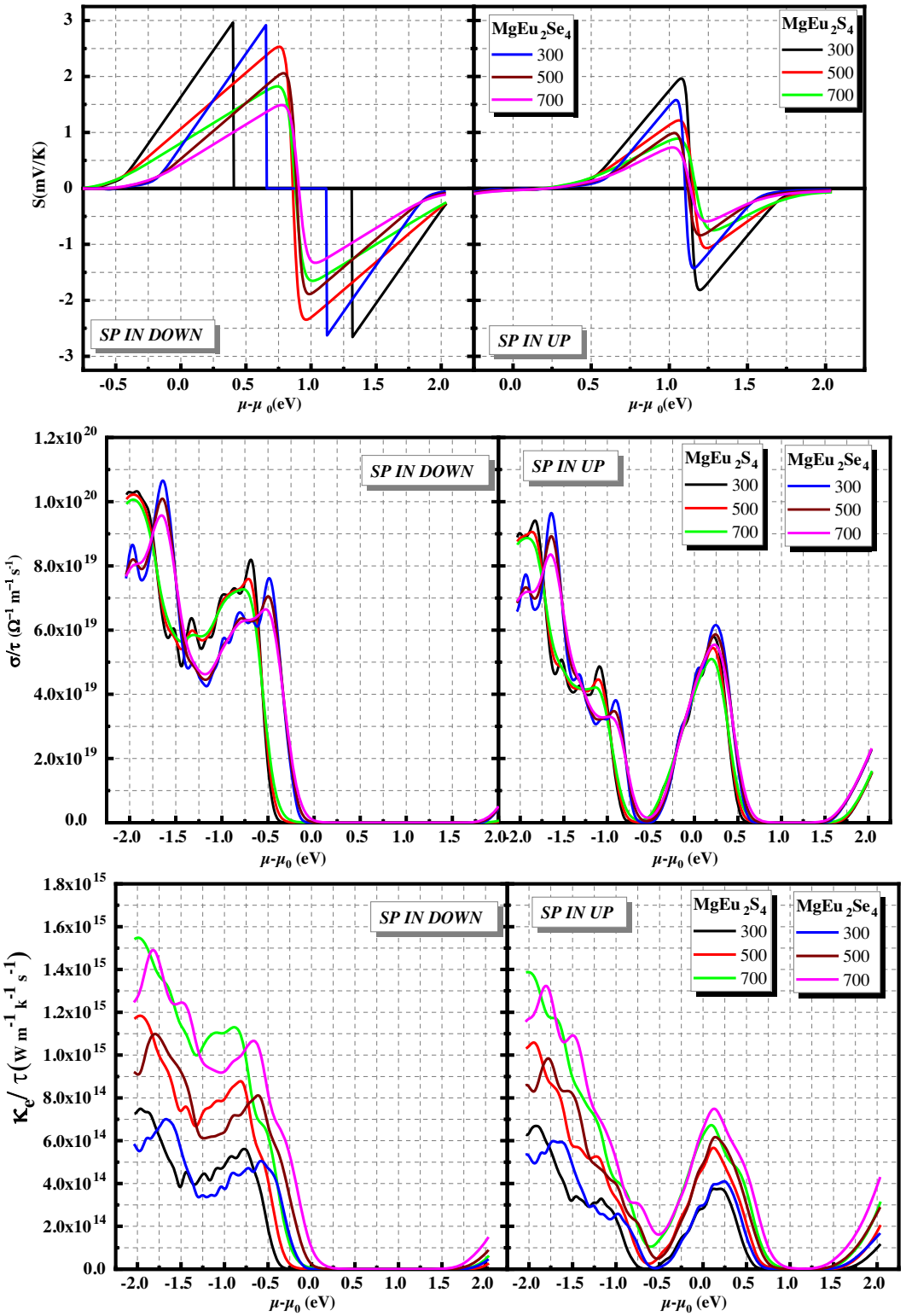

Figure 8. Variation of Seebeck coefficients, electrical conductivity and electronic thermal conductivity as function of relative chemical potential of $MgEu_2Se_4$ and $MgEu_2S_4$ in both spin channels.

in the range [−1.5; −1] eV in the case of spin down. In the spin-down case, one can also notice the effect of temperature on these two electronic heat capacity coefficients, where the electronic heat capacity increases as the temperature increases. As for the changes in Pauli magnetic susceptibility for both compounds, which are plotted in Figure 9, we found that the magnetic susceptibility takes its maximum values in the range (−0.5 − 0) eV in the spin-up case and it is inversely proportional with the increase of the temperature.

To know if these two compounds are suitable for use in the thermoelectric field, either as thermal sensors or in thermoelectric generators, we can refer to the figure of merit ZT ($ZT = \frac{S^2\sigma T}{\kappa}$ where S is the Seebeck coefficient, σ is the electrical conductivity, $\kappa = \kappa_e + \kappa_l$ is the total thermal conductivity, and T is the absolute temperature) and the power factor (PF $= S^2{\cdot}\sigma$) criterions, where these two parameters have been calculated and plotted in **Figure 10**. Through this figure, it can be noticed that the $MgEu_2S_4$ has a higher power factor (PF) than $MgEu_2Se_4$, and that the values of this coefficient of both compounds in the case of spin down are higher than in the case of spin up, in addition to the direct proportionality between this coefficient and temperature. Regarding the coefficient of merit ZT, we note that both compounds have similar values set up to 0.55 at $T = 300$ K in spin-down direction, and this coefficient is also directly proportional to temperature and rises to 0.83 for both compounds at $T = 700$ K; whereas the value of this parameter did not exceed 0.5 in the case of spin up at room temperature.

The different thermoelectric parameters of both $MgEu_2S_4$ and $MgEu_2Se_4$ are calculated at the Fermi level for each compound and plotted in **Figures 11** and **12**. From the reported curves in Figure 11, the maximum values of the Seebeck coefficient reached at 100 and 200 K for $MgEu_2Se_4$ and $MgEu_2S_4$, respectively, in the case of spin down, and its decrease with the increase of temperature above these two temperatures values, however in the case of spin up, they have negative values and almost null.

Regarding the evolution of electrical conductivity and electronic thermal conductivity estimated in the two spin cases in terms of temperature changes shown in Figure 11, we recorded an increase of electronic thermal conductivity with increasing temperature in the spin-up case, while the electrical conductivity decreases with increasing temperature, and in the case of the spin down that shown in Figure 11, the electrical and the thermal conductivities have similar shapes so the electrical conductivity has negligible values and is equal to zero at low temperature for both compounds, as it starts to increase significantly and has an exponential coefficient for $MgEu_2Se_4$ from a temperature of 300 K, while it takes low values and with an exponential coefficient from the temperature of 600 For $MgEu_2Se_4$. According to

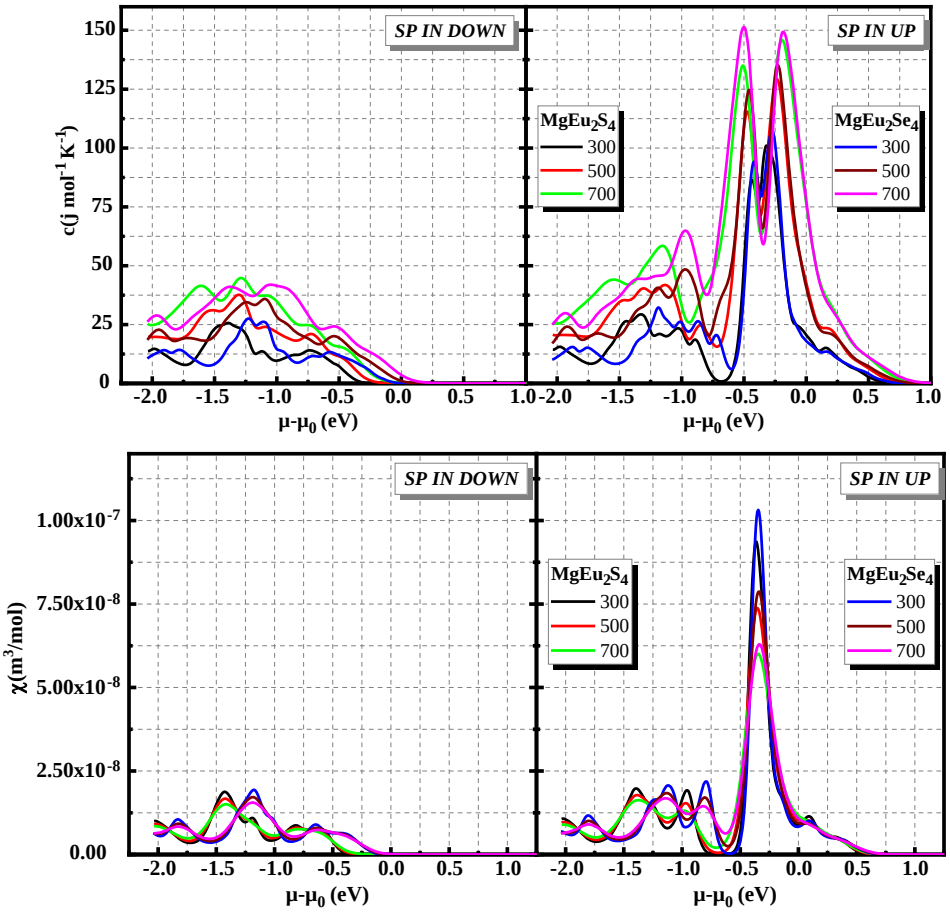

Figure 9. Variation of electronic heat capacity and Pauli magnetic susceptibility as a function of relative chemical potential of $MgEu_2Se_4$ and $MgEu_2S_4$ in both spin channels.

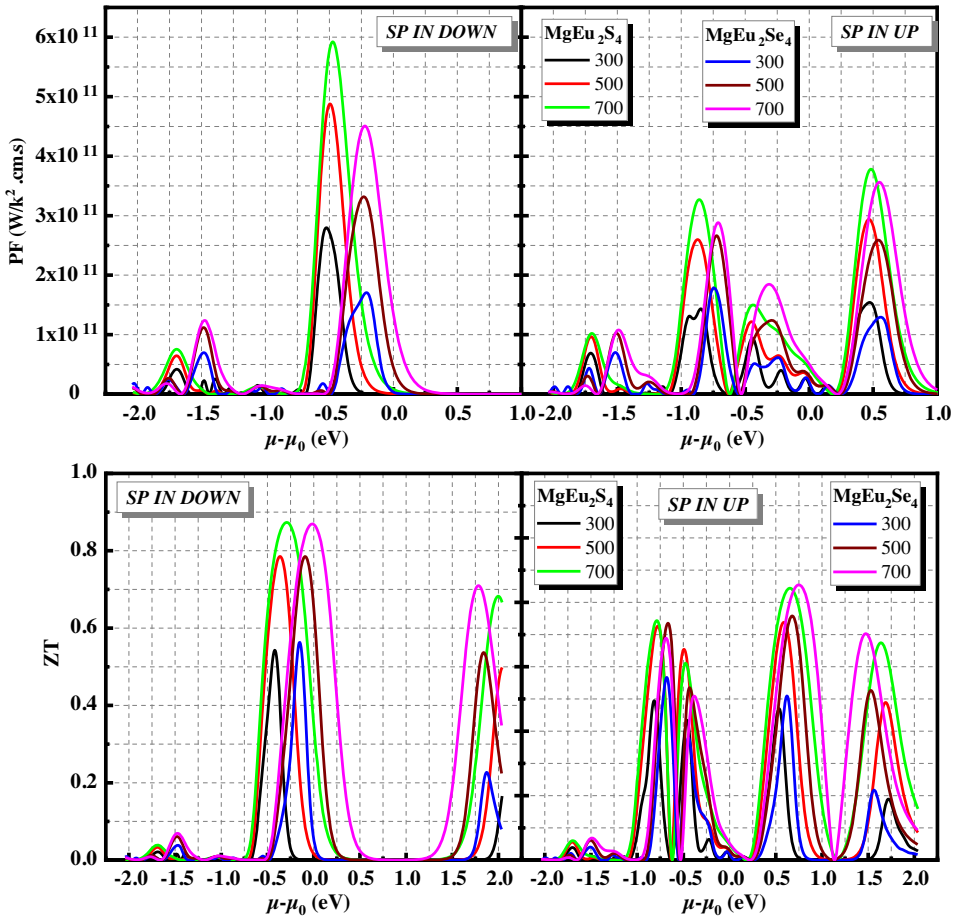

Figure 10. Variation of the figure of merit ZT and power factor (PF) as a function of relative chemical potential of $MgEu_2Se_4$ and $MgEu_2S_4$ in both spin channels.

Figure 11, the electronic heat capacity calculated at the Fermi level increases near-linearly in the spin-up case for both compounds, while in the spin-down case it starts to increase at 250 K for $MgEu_2Se_4$ and 550 K for $MgEu_2S_4$.

As for the ZT and the PF calculated at the ground case and plotted in Figure 12, it was found that these two coefficients increased with temperature and have almost negligible values in the case of spin up compared to spin down at temperature greater than 300 K, where in the spin-down direction these two coefficients have zero value for temperature lower than 200 and 500 K for $MgEu_2S_4$ and $MgEu_2Se_4$, respectively, and they increase with the increase of the temperature beginning from 250 K for $MgEu_2Se_4$ and slightly from 550 K for $MgEu_2S_4$ compound in spin-down case. In spin down, the power factor (PF) and ZT of $MgEu_2Se_4$ increase rapidly and dramatically after room temperature whereas in the case of $MgEu_2S_4$ they increase less after 550 K. In contrast, upon spin up, both spinels have a similar trend evolution.

4. Conclusions

Ab-initio calculations are used to investigate the structural, elastic, electronic, and thermoelectric properties of the $MgEu_2X_4$ (X = S and Se) spinel compounds. In these calculations, it is shown that these two compounds have a half-metallic character in a minority channel with a direct (Γ-Γ) energy bandgap (E_g) and they have a value of 3.44, 2.712, and 2.472 eV for $MgEu_2S_4$ and 2.893, 2.285, and 2.017 eV for $MgEu_2Se_4$. In addition, both compounds have a high total spin magnetic moment (12 μ_B). These high magnetic moments make both compounds potential candidates for magnetocaloric applications. Investigation of the mechanical and elastic properties showed that all the studied compounds are mechanically stable and classifying these compounds as ductile anisotropic materials. The chemical bonding for both spinels is of mixed ionic- covalent type formed by ionic Mg–Eu and covalent–ionic Mg–S/Se bonds. The main conclusion from this study about thermoelectric properties is that the spin-down ZT value of $MgEu_2Se_4$ spinel increases dramatically from 0.05 at 300 K to reach about 0.9 at 800 K, whereas the spin-down ZT value of $MgEu_2S_4$ start to increase after 550 K to reach 0.6 at 800 K. In contrast, it was found that the Seebeck coefficient is affected directly by temperature changes and decreases with increasing temperature for both compounds and in both spins. The Seebeck coefficient in the spin-down channel is larger than in the other channel for both compounds with maxima of 2.5 mV K^{-1} at 200 K for $MgEu_2S_4$ and 1.85 mV K^{-1} at 100 K for

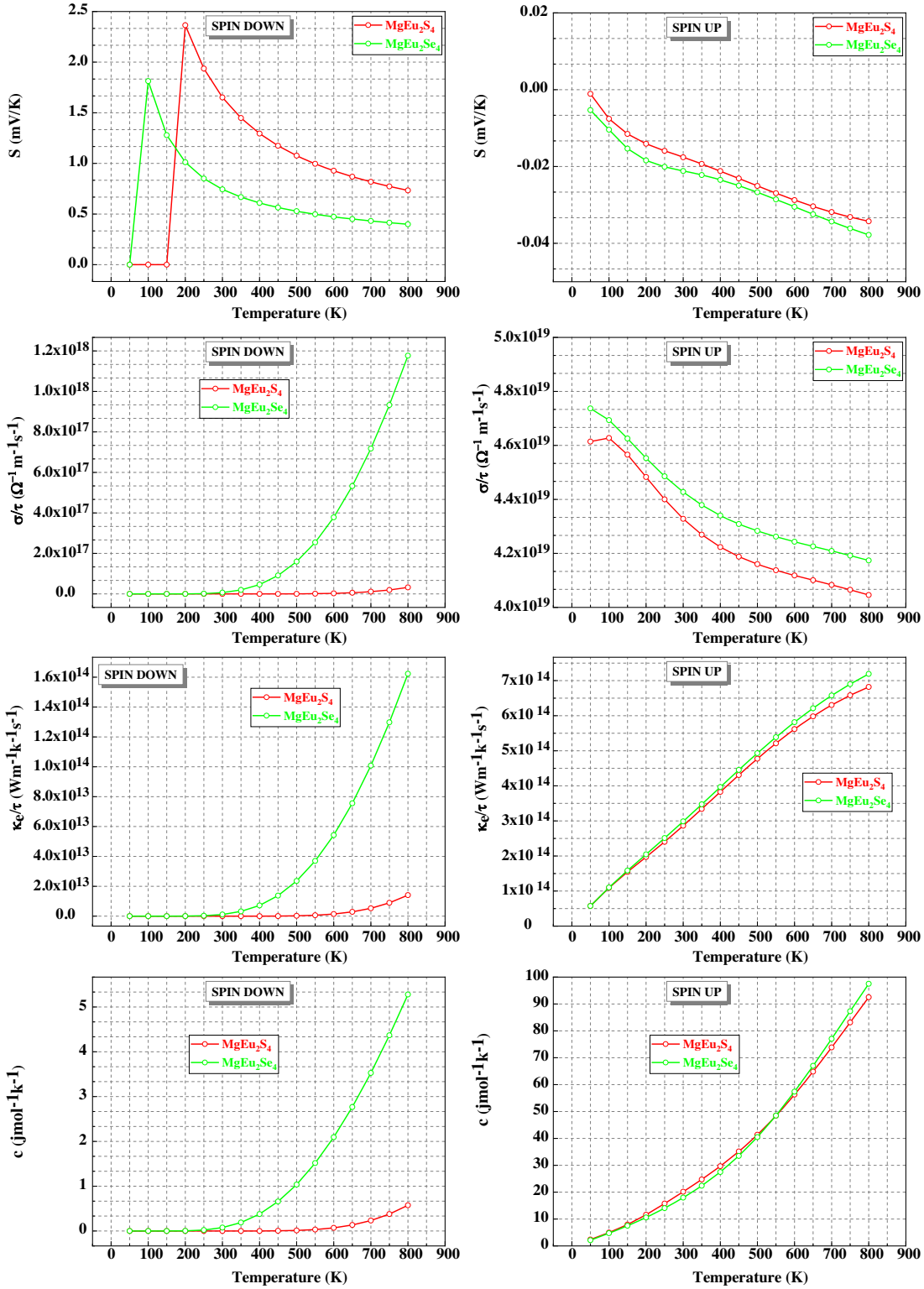

Figure 11. Temperature dependence of Seebeck coefficient, electronic heat capacity, electrical conductivity, and electronic thermal conductivity at the ground state chemical potential for $MgEu_2Se_4$ and $MgEu_2S_4$ in both spin channels.

$MgEu_2Se_4$. At the normal pressure and temperature conditions, the study of the thermal behavior demonstrates that $MgEu_2Se_4$ has a larger coefficient of thermal expansion and heat capacity than $MgEu_2S_4$.

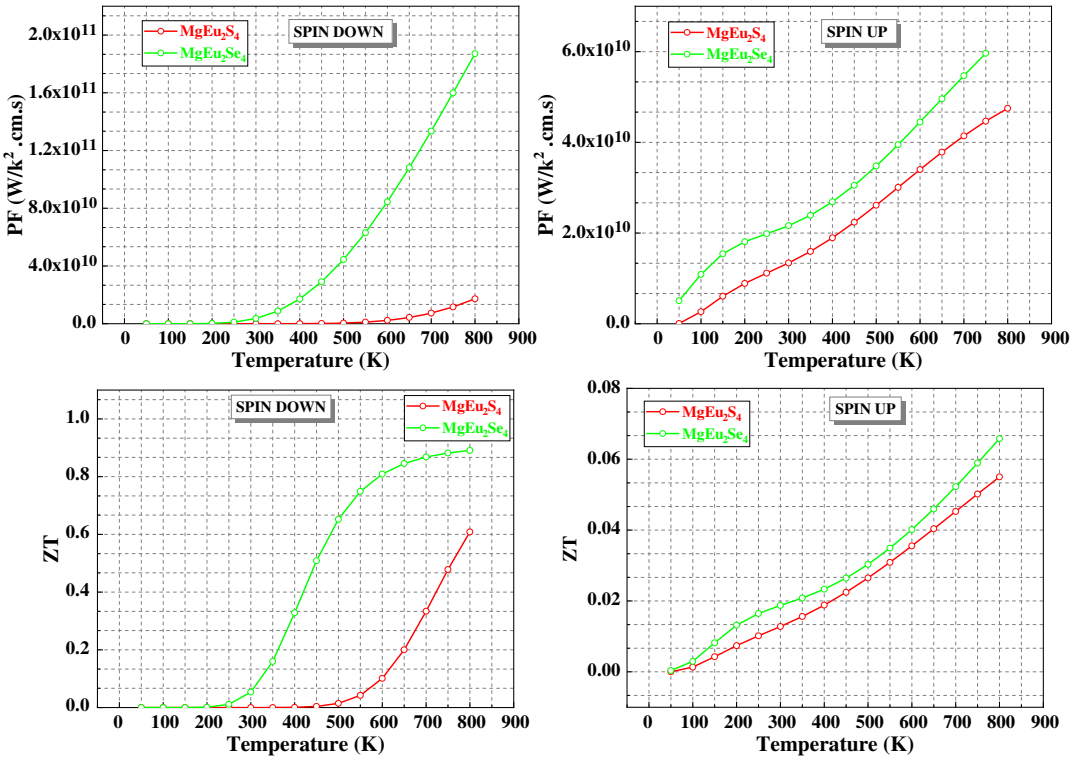

Figure 12. Temperature dependence of the figure of merit *ZT* and power factor (PF) at the ground state chemical potential for $MgEu_2Se_4$ and $MgEu_2S_4$ in both spin channels.

Conflict of Interest

The authors declare no conflict of interest.

Data Availability Statement

The data that support the findings of this study are available from the corresponding author upon reasonable request.

Keywords

half-metallic, Seebeck coefficient, spinel, thermal expansion, thermoelectric

Received: April 30, 2022
Revised: July 6, 2022
Published online: August 2, 2022

[1] M. Patrie, L. Domange, J. Flahaut, *C. R. Hebd. Seances Acad. Sci.* **1964** *258*, 2585.
[2] M. Guittard, C. Souleau, H. Farsam, *C. R. Hebd. Seances Acad. Sci.* **1964** *259*, 2847.
[3] A. Williams, T. McQueen, R. Cava, *Solid State Commun.* **2009**, *149*, 1507.
[4] a) The Materials Project. Materials Data on Eu_2MgS_4 by Materials Project. United States **2020**, https://doi.org/10.17188/1743316; b) The Materials Project. Materials Data on Eu_2MgSe_4 by Materials Project. United States **2020**, https://doi.org/10.17188/1758623.
[5] Y. Wang, W. Chen, F. Liu, D. Yang, Y. Tian, C. Ma, M. Dramićanin, M. Brik, *Physics* **2019**, *13*, 102180.
[6] J. Koettgen, C. J. Bartel, G. Ceder, *Chem. Commun.* **2020**, *56*, 1952.
[7] S. Al-Qaisi, D. Rai, T. Alshahrani, R. Ahmed, B. Ul Haq, S. Tahir, M. Khuili, Q. Mahmood, *Mater. Sci. Semicon. Proc.* **2021**, *128*, 105766.
[8] L. Idrissi, N. Tahiri, O. El Bounagui, H. Ez-Zahraouy, *J. Supercond. Nov. Magn.* **2020**, *33*, 1369.
[9] L. Idrissi, N. Tahiri, O. El Bounagui, *Phase Transit.* **2021**, *94*, 134.
[10] H. Jebari, N. Tahiri, M. Boujnah, O. El Bounagui, M. Taibi, N. Tahiri, M. Boujnah, O. El Bounagui, M. Taibi, *Phase Transit.* **2021**, *94*, 147.
[11] G. Kadim, R. Masrour, A. Jabar, *J. Magn. Magn. Mater.* **2020**, *499*, 166263.
[12] R. Masrour, A. Jabar, E. K. Hlil, M. Hamedoun, A. Benyoussef, A. Hourmatallah, *J. Magn. Magn. Mater.* **2017**, *430*, 89.
[13] A. El Grini, M. Hamedoun, A. Benyoussef, R. Masrour, O. Mounkachi, A. Hourmatallah, N. Benzakour, K. Bouslykhane, *Phase Transit.* **2013**, *86*, 1186.
[14] S. Salmi, R. Masrour, A. Jabar, A. El Grini, A. Azouaoui, K. Bouslykhane, A. Hourmatallah, N. Benzakour, M. Hamedoun, *Chem. Phys.* **2021**, *547*, 111195.
[15] A. El Maazouzi, R. Masrour, A. Jabar, *J. Cryst. Growth* **2022**, *584*, 126552.
[16] R. Masrour, E. K. Hlil, M. Hamedoun, A. Benyoussef, O. Mounkachi, *J. Magn. Magn. Mater.* **2014**, *378*, 37.
[17] D. D. Koelling, B. N. Harmon, *J. Phys. C: Solid State Phys.* **1977**, *10*, 3107.
[18] P. Hohenberg, W. Kohn, *Phys. Rev. B* **1964**, *136*, 864.
[19] P. Blaha, K. Schwarz, F. Tran, R. Laskowski, G. K. H. Madsen, L. D. Marks *J. Chem. Phys.* **2020** *152*, 074101.
[20] F. D. Murnaghan, *Proc. Natl. Acad. Sci. USA* **1944**, *30*, 244.

[21] J. P. Perdew, K. Burke, M. Ernzerhof, *Phys. Rev. Lett.* **1996**, *77*, 3865.
[22] V. I. Anisimov, O. Gunnarsson, *Phys. Rev. B* **1991**, *43*, 7570.
[23] V. I. Anisimov, J. Zaanen, O. K. Andersen, *Phys. Rev. B* **1991**, *44*, 943.
[24] F. Tran, P. Blaha, *Phys. Rev. Lett.* **2009**, *102*, 226401.
[25] F. Nejadsattari, Z. M. Stadnik, *Sci. Rep.* **2021**, *11*, 12113.
[26] M. Alrahamneh, A. Mousa, J. Khalifeh, *Physica B* **2019**, *552*, 227.
[27] M. Alrahamneh, *Physica B* **2020**, *581*, 411941.
[28] M. Jamal, IRelast and 2DR-optimize packages are provided by M. Jamal as part of the commercial code WIEN2k, **2014**.
[29] M. Jamal, M. Bilal, I. Ahmad, S. Jalali-Asadabadi, *J. Alloys Compd.* **2018**, *735*, 569.
[30] M. Born, K. Huang, in *Dynamical Theory of Crystal Lattice*, Clarendon Press, Oxford, UK **1954**.
[31] A. Mousa, R. Jaradat, S. M. Azar, M. Abu-Jafar, E. K. Jaradat, J. Khalifeh, K. Ilaiwi, *Chin. J. Phys.* **2019**, *29*, 210.
[32] V. Tvergaard, J. Hutshinson, *J. Am. Ceram. Soc.* **1988**, *71*, 157.
[33] P. Ravindran, L. Fast, P. Korzhavyi, B. Johansson, *J. Appl. Phys.* **1998**, *84*, 4891.
[34] A. A. Mousa, M. S. Abu-Jafar, D. Dahlilah, R. M. Shaltah, J. M. Khalifeh, *J. Electron. Mater.* **2018**, *47*, 641.
[35] R. Hill, *Proc. Phys. Soc. Lond. A* **1952**, *65*, 349.
[36] W. Voigt, *Ann. Phys. (Leipzig)* **1889**, *38*, 573.
[37] A. Reuss, *Z. Angew. Math. Phys.* **1929**, *9*, 49.
[38] D. Teter, *MRS Bull.* **2013**, *23*, 22.
[39] S. F. Pugh, *Philos. Mag.* **1954**, *45*, 823.
[40] D. Pettifor, *Mater. Sci. Technol.* **1992**, *8*, 345.
[41] I. Frantsevich, F. Voronov, S. Bokuta, in *Elastic Constants and Elastic Moduli of Metals and Insulators Handbook*, Naukova Dumka, Kiev, Ukraine **1983**, p. 60.
[42] M. Jamal, S. Asadabadi, I. Ahmad, H. Aliabad, *Comput. Mater. Sci.* **2014**, *95*, 592.
[43] S. Azar, B. Hamad, J. Khalifeh, *J. Magn. Magn. Mater.* **2012**, *324*, 1776.
[44] S. M. Azar, A. A. Mousa, K. J. M. Structural, *Intermetallics* **2017**, *85*, 197.
[45] A. Otero-de-la-Roza, D. Abbasi-Pérez, V. Luaña, *Comput. Phys. Commun.* **2011**, *182*, 2232.
[46] A. Otero-de-la-Roza, V. Luaña, *Comput. Phys. Commun.* **2011**, *182*, 1708.
[47] P. Debye, *Ann. Phys. (Leipzig)* **1926**, *386*, 1154.
[48] S. Essaoud, A. Jbara, *J. Magn. Magn. Mater.* **2021**, *531*, 167984.
[49] P. L. Dulong, A.-T. Petit, Recherches sur quelques points importants de la theorie de la chaleur, *Ann. Chim. Phys.* **1819**, *10*, 395.
[50] G. Slack, *J. Phys. Chem. Solids* **1973**, *34*, 321.
[51] G. Madsen, D. Singh, *Comput. Phys. Commun.* **2006**, *175*, 67.